A role for the Rb family of proteins in controlling telomere length

Marta García-Cao[1], Susana Gonzalo[2], Douglas Dean[2] & María A. Blasco[1]

Published online 15 October 2002; doi:10.1038/ng1011

The molecular mechanisms of cellular mortality have recently begun to be unraveled. In particular, it has been discovered that cells that lack telomerase are subject to telomere attrition with each round of replication, eventually leading to loss of telomere capping function at chromosome ends[1–5]. Critically short telomeres and telomeres lacking telomere-binding proteins lose their functionality and are metabolized as DNA breaks, thus generating chromosomal fusions[1–8]. Telomerase activity is sufficient to rescue short telomeres and confers an unlimited proliferative capacity[9–11]. In addition, the tumor-suppressor pathway Cdkn2a/Rb1 has also been implicated as a barrier to immortalization[12–14]. Here, we report a connection between the members of the retinoblastoma family of proteins, Rb1 (retinoblastoma 1), Rbl1 (retinoblastoma-like 1) and Rbl2 (retinoblastoma-like 2), and the mechanisms that regulate telomere length. In particular, mouse embryonic fibroblasts doubly deficient in *Rbl1* and *Rbl2* or triply deficient in *Rbl1*, *Rbl2* and *Rb1* have markedly elongated telomeres compared with those of wildtype or *Rb1*-deficient cells. This deregulation of telomere length is not associated with increased telomerase activity. Notably, the abnormally elongated telomeres in doubly or triply deficient cells retain their end-capping function, as shown by the normal frequency of chromosomal fusions. These findings demonstrate a connection between the Rb1 family and the control of telomere length in mammalian cells.

To investigate the role of the members of the Rb1 family in controlling telomere length, we measured telomere length in primary mouse embryonic fibroblasts (MEFs) with the genotypes $Rb1^{-/-}$, $Rbl1^{-/-}$ $Rbl2^{-/-}$ (DKO) and $Rb1^{-/-}$ $Rbl1^{-/-}$ $Rbl2^{-/-}$ (TKO) and in wildtype controls[15]. First, we used terminal restriction fragment (TRF) analysis to estimate telomere length[7]. Early-passage $Rb1^{+/+}$ and $Rb1^{-/-}$ MEFs showed TRFs of similar sizes, indicating that Rb1 deficiency did not alter telomere length (Fig. 1*a*). Notably, both DKO and TKO MEFs had larger TRFs than did the corresponding wildtype controls, suggesting a 'long-telomere' phenotype in these cells (Fig. 1*a*). The telomere elongation was more pronounced in TKO cells than in DKO cells. The fact that the elongated telomeres of DKO and TKO cells were not observed in any of the $Rb1^{-/-}$ MEFs that we studied suggests that the long-telomere phenotype is specifically associated with deficiency in *Rbl1*, *Rbl2* or both, but not with deficiency in *Rb1* alone. We cannot, however, rule out the possibility that deficiency in *Rb1* combined with deficiency in either *Rbl1* or *Rbl2* may have an effect on telomere length—DKO primary MEFs with functional Rb1 protein showed elongated telomeres at the earliest passage studied (passage (p) 1), whereas TKO MEFs at a similar passage, which lack Rb1, showed two distinct populations with either normal-length or elongated telomeres (Fig. 1*a*). At later passages (p8 for TKO-B, p20 for TKO-C), however, most of the telomeres seemed to be elongated in TKO cells (Fig. 1*a*).

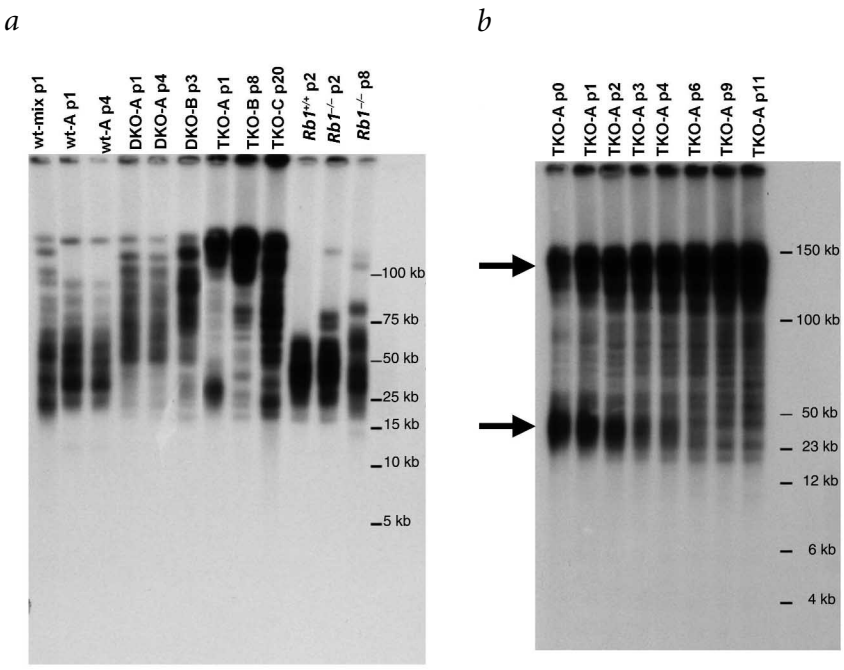

Fig. 1 Deregulation of telomere length in DKO and TKO cells. ***a***, Representative TRF analysis of wildtype MEFs and several independent $Rb1^{-/-}$, DKO and TKO MEFs at different passages. DKO and TKO MEFs had higher-molecular-weight TRF fragments than did the corresponding wildtype cells. Letters denote independent MEF cultures. ***b***, TRF analysis of TKO MEFs at different passages using the 3T3 protocol. There was a shift toward larger TRF fragments in later passages compared with earlier passages.

[1]*Department of Immunology and Oncology, National Center of Biotechnology, E-28049 Madrid, Spain.* [2]*Division of Molecular Oncology, Washington University School of Medicine, St. Louis, Missouri, USA. Correspondence should be addressed to M.A.B. (e-mail: mblasco@cnb.uam.es).*

We took advantage of the fact that TKO primary MEFs are immortal and do not show senescence-like arrest[15] to investigate telomere dynamics at increasing passages. As TKO MEFs accumulated passages, the population having normal-length telomeres decreased concomitantly with an increase in the population having elongated telomeres (Fig. 1*b*). This switch from normal to long telomeres occurred rapidly, and most of the telomeres of TKO MEFs were elongated at p6 (Fig. 1*b*).

To determine whether changes in telomere length occurred within the same nucleus or were due to the existence of two different cell populations in the TKO MEFs, we carried out quantitative fluorescence *in situ* hybridization (Q-FISH) of metaphase nuclei using a telomere-specific probe. Telomere-length histograms of early-passage TKO MEFs (TKO-A p1; Fig. 2*a*,*b*) showed two peaks corresponding to normal and long telomeres, with average lengths of 33.9 ± 12.3 kb and 87.0 ± 26.9 kb, respectively (data are mean ± s.d.; Table 1).

Early-passage $Rb1^{-/-}$ MEFs (p2) showed a telomere length distribution similar to that of $Rb1^{+/+}$ MEFs (Fig. 2*a*), with average lengths of 45.2 ± 15.8 kb and 42.9 ± 14.2 kb, respectively (Table 1). Increasing passages of the $Rb1^{-/-}$ cells (up to p8) did not show telomere shortening, in agreement with telomerase activity in these cells (Table 1). In contrast, early-passage DKO MEFs (DKO-A p1) had significantly longer telomeres than did wildtype controls (wt-A p1; $P < 0.0001$; Fig. 2*a*), with average lengths of 61.3 ± 18 kb and 44.5 ± 15.4 kb, respectively (Table 1). Increasing passages of two independent DKO MEFs (DKO-A p2, DKO-A p4 and DKO-B p3) also showed elongated telomeres compared to wildtype controls at similar passages (Fig. 2*a*, Table 1). Therefore, DKO MEFs showed a long-telomere phenotype at the earliest passage studied, which was maintained with increasing passages.

Notably, as TKO cells accumulated passages, the percentage of metaphases with normal-length telomeres decreased from 87% at p0 to 0% at p9 (Tables 1 and 3). Two additional TKO MEF cultures, TKO-B and TKO-C, also showed rapid telomere elongation, reaching lengths similar to those found for the TKO-A MEF culture (Fig. 2*a*, Table 1). These results indicate that in TKO MEFs, a rapid selection of cells with deregulated telomere length occurs with passaging. Although TKO MEFs behave as immortal, there was a modest but reproducible increase in cell death at early passages (p4–6) that disappeared after p6–9, coincidental with a selection of cells with a smaller-sized morphology (data not

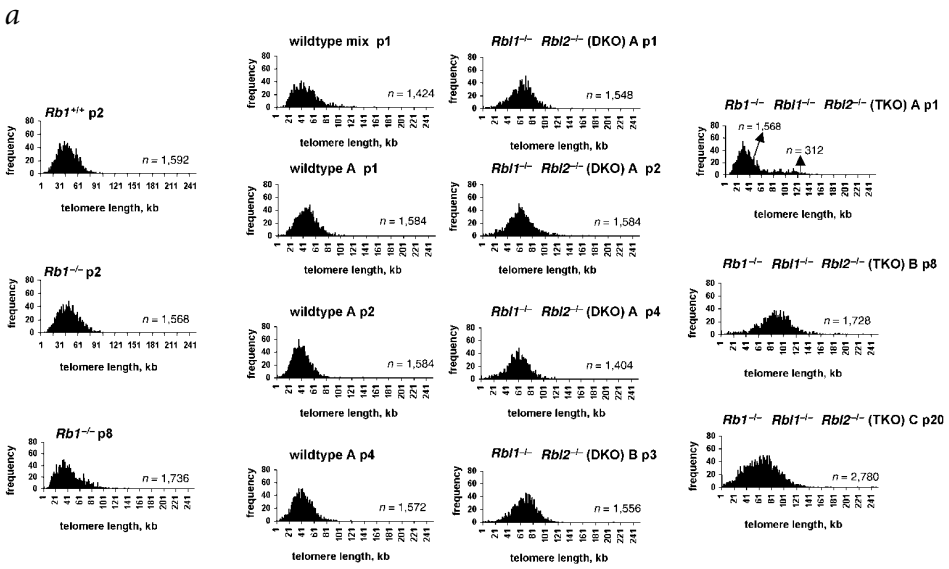

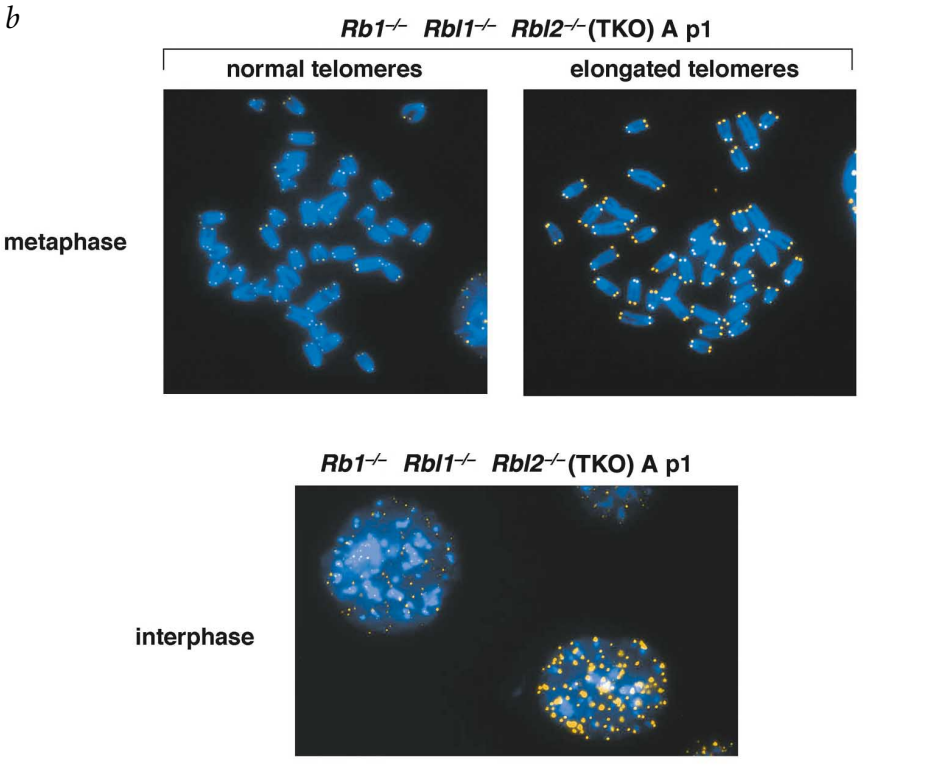

Fig. 2 Abnormally elongated telomeres in DKO and TKO cells as determined by Q-FISH. ***a***, Telomere-length distribution of $Rb1^{-/-}$, $Rb1^{+/+}$, DKO, TKO and wildtype MEFs. In early-passage TKO MEFs, two peaks corresponding to normal-length and elongated telomeres were observed. *n*, total number of telomeres analyzed from each MEF. Letters denote independent MEF cultures. ***b***, Representative Q-FISH images of metaphase and interphase nuclei from TKO MEFs. Telomere fluorescence is indicated by yellow dots.

Table 1 • Telomere lengths in MEF cultures of different genotypes as determined by Q-FISH

Genotype	p arm, kb	q arm, kb	Average p+q, kb	Metaphases analyzed	Number of telomeres	% undetectable telomeres
Rb1$^{+/+}$ p2	38.3 ± 13.4	47.7 ± 15.0	42.9 ± 14.2	10	1,592	0
Rb1$^{-/-}$ p2	41.1 ± 15.2	49.4 ± 16.4	45.2 ± 15.8	10	1,568	0
Rb1$^{-/-}$ p8	34.1 ± 13.9	50.5 ± 23.0	42.3 ± 18.5	10	1,736	0.17
wt-mix p1	39.8 ± 17.4	51.3 ± 19.4	45.5 ± 18.4	10	1,424	0.07
wt-A p1	39.9 ± 14.7	49.0 ± 15.9	44.5 ± 15.4	10	1,584	0.13
wt-A p2	35.6 ± 13.9	41.4 ± 13.9	38.5 ± 13.9	10	1,584	0.25
wt-A p4	37.1 ± 14.2	44.2 ± 14.8	40.7 ± 14.5	10	1,572	0.06
DKO-A p1	56.2 ± 15.1	66.5 ± 30.0	61.3 ± 18.0	10	1,548	0.26
DKO-A p2	54.3 ± 16.9	65.2 ± 22.4	59.7 ± 19.6	10	1,584	0.19
DKO-A p4	52.4 ± 15.0	63.7 ± 19.1	58.1 ± 17.1	10	1,404	0.28
DKO-B p3	60.4 ± 16.2	71.1 ± 20.0	65.7 ± 18.1	10	1,556	0.13
TKO-A p1[a]	27.8 ± 9.8	40.2 ± 14.9	33.9 ± 12.3	10	1,568	0.45
	76.5 ± 24.3	97.8 ± 29.6	87.0 ± 26.9	2	312	0
TKO-A p2[a]	29.4 ± 11.3	44.1 ± 16.2	36.8 ± 13.8	10	1,579	0.38
	69.6 ± 27.4	110.6 ± 32.6	90.1 ± 29.9	3	453	0.22
TKO-A p4[a]	22.1 ± 10.7	37.0 ± 14.2	29.6 ± 12.5	10	1,740	0.98
	77.3 ± 31.0	107.2 ± 36.8	92.3 ± 33.6	10	1,388	0.58
TKO-A p6[a]	25.3 ± 15.5	38.7 ± 15.2	32.0 ± 14.4	10	1,532	1.11
	75.8 ± 31.7	111.5 ± 42.4	93.6 ± 37.0	10	1,836	0.65
TKO-A p11[b]	–	–	–	0	0	–
	77.8 ± 37.3	114.9 ± 78.9	96.3 ± 58.1	10	1,856	0.86
TKO-B p8	77.3 ± 22.8	95.2 ± 31.1	86.2 ± 26.9	10	1,728	0.29
TKO-C p20	74.8 ± 45.3	98.6 ± 42.6	86.7 ± 44.0	10	2,780	0.68

[a]Telomere length was determined for both the population of cells with normal telomeres (top row) and that with long telomeres (bottom row). [b]Only metaphases with long telomeres were present.

shown). Our results suggest that those TKO cells that are selected with passaging and that are immortal also show deregulated telomere length. It is important to note that the disappearance of cells with normal telomeres from the TKO MEF cultures was not a result of extreme telomere shortening with increasing passages in these cells (Table 1). The long-telomere phenotype of the TKO cells was probably not responsible for their immortality, as primary DKO cells, which also showed elongated telomeres, were not immortal and showed the typical senescence-like arrest after 5–10 population doublings in culture[15]. It was the additional loss of Rb1 that seemed to permit TKO MEFs with abnormally elongated telomeres to divide immortally.

We next examined whether the long telomeres of DKO and TKO cells retained their end-capping function by measuring the frequency of end-to-end chromosomal fusions, which result from dysfunctional telomeres[7,16–19]. We classified end-to-end fusions into those that involve the p arms of chromosomes (robertsonian-like fusions) and those that involve the q arms (dicentric fusions). Q-FISH analysis of each MEF showed no robertsonian-like fusions and low frequencies of dicentric fusions, suggesting that telomeres were functional (Table 2). In addition, none of the MEFs that we studied showed markedly higher frequencies of undetectable telomeres (TTAGGG signal-free ends; Table 1, Fig. 2*a*), another hallmark of telomere dysfunction[9,10]. Accumulation of passages in TKO cells did not result in dysfunctional telomeres either, as indicated by the low percentage of undetectable telomeres and by the low frequency of end-to-end fusions (Tables 1 and 3).

A complementary way to study telomere integrity is to test the binding of TTAGGG-binding proteins, such as Terf1 (ref. 20), to the telomeres. Binding of Terf1 to the telomere is proportional to the length of TTAGGG repeats[21–23]. We studied binding of Terf1 to the telomeres by immunofluorescence on interphase nuclei. Late-passage TKO cells (TKO-C p20) showed significantly greater Terf1 fluorescence per interphase telomere than did wild-type controls (734.8 ± 381.3 and 421.8 ± 233.5 arbitrary units of fluorescence, respectively; $P = 3.5 \times 10^{-5}$), suggesting that more Terf1 molecules were bound to TKO telomeres, in agreement with elongated telomeres in these cells (Fig. 3). Late-passage TKO cells also showed more Terf1 spots per interphase nucleus (Fig. 3*b*), probably reflecting the fact that these cells are aneuploid (S.G., M.G.-C., R. Eguía, S. Cotter, T. Jenuwein, M.A.B. and D.C.D., unpublished results).

Table 2 • Frequency of chromosomal aberrations per metaphase in *Rb1*$^{-/-}$, *Rb1*$^{+/+}$, DKO, TKO and wildtype MEFs

Genotype	Number of metaphases	Telomere fusions (dicentric)	Telomere fusions (robertsonian-like)
wt-mix p1	50	0	0
wt-A p1	50	0	0
wt-A p2	50	0	0
wt-A p4	50	0	0
DKO-A p1	50	0	0
DKO-A p2	40	0	0
DKO-A p4	50	0	0
DKO-B p3	50	0	0
TKO-A p1	50	0.040	0
TKO-B p8	50	0	0
TKO-C p20	50	0.025	0
Rb1$^{+/+}$ p2	50	0	0
Rb1$^{-/-}$ p2	50	0	0
Rb1$^{-/-}$ p8	50	0	0

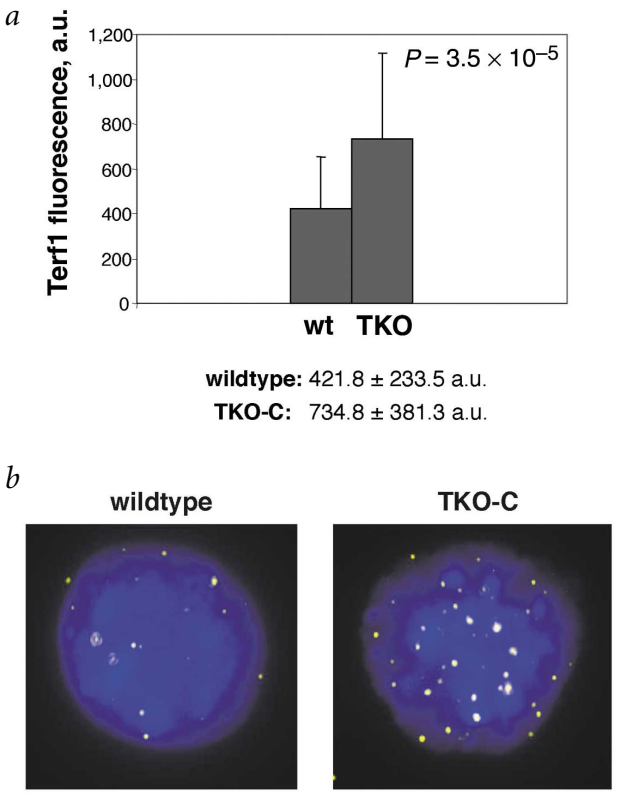

Fig. 3 Greater binding of Terf1 to TKO telomeres. ***a***, Average Terf1 fluorescence (in arbitrary units, a.u.) of interphase telomeres as determined by Q-FISH. Terf1 fluorescence was significantly greater in TKO than in wildtype (wt) cells, as indicated by a Student's *t*-test ($P = 3.5 \times 10^{-5}$). We analyzed more than 40 nuclei for each genotype. ***b***, Representative images of Terf1 spots (yellow) in DAPI-stained interphase nuclei (blue). Terf1 signals (yellow) were more intense in TKO than in wildtype cells.

To address whether the effect on telomere length was a result of changes in telomerase expression, we carried out telomeric repeat amplification assays. All the genotypes that we studied showed similar levels of telomerase activity at different passages (data not shown), suggesting that the long-telomere phenotype was not associated with changes in telomerase activity. We cannot, however, rule out the possibility that the accessibility of the telomere to telomerase was altered in DKO and TKO cells, as recently shown for *Xrcc5*-deficient cells[23]. The access of telomerase to the telomere could be influenced, for instance, by the status of the telomeric chromatin. Alternatively, DKO and TKO cells could have activated mechanisms for telomerase-independent telomere elongation, known as alternative lengthening of telomeres[24], that could co-exist with telomerase activity[25]. In this regard, it is relevant to note that late-passage TKO cells have long and heterogeneous telomeres (Fig. 1*a*), a hallmark of activation of alternative lengthening of telomeres[24].

The results presented here indicate that members of the Rb1 protein family are key regulators of telomere length in mammalian cells. This finding links, for the first time, the regulation of telomere length with cell-cycle control. It is possible that the Rb1 family members could have a direct role in regulating telomere length or telomere structure independent of their role in cell-cycle regulation. Notably, disruption of members of the Rb1 pathway results in rapid telomere elongation, which, in turn, may help to sustain immortal or tumor growth. This finding could be the basis for the lifespan extension exerted by a number of viral oncoproteins that inactivate the Rb1 family.

Methods

Cells. We used a mixed C57BL/6–129/Sv genetic background for the DKO and TKO MEFs as previously described[15]. For some genotypes, we used several independent MEF cultures, denoted as A, B and/or C. In all experiments, we matched the DKO and TKO MEFs with wildtype MEFs of a similar genetic background[26]. Wildtype MEFs from a different mixed genetic background (C57BL/6J–129/Sv–SJL; ref. 7) were also included where indicated; these MEFs are named wt-mix. Telomere length in wildtype MEFs from either mixed genetic background was similar. The genetic background of the $Rb1^{-/-}$ and $Rb1^{+/+}$ MEFs was a pure C57BL/6J genetic background (JAXMICE, strain name B6.129S2-Rb1, stock 002102). We carried out the 3T3 passaging protocol as described[7]. The earliest passage after MEFs isolation was considered p1.

Telomere length measurements. We carried out TRF analysis and Q-FISH hybridization as previously described[7,17]. To correct for lamp intensity and alignment, we analyzed images from fluorescent beads (Molecular Probes) using the TFL-Telo program (gift from P. Lansdorp). Telomere fluorescence values were extrapolated from the telomere fluorescence of lymphoma cell lines LY-R (R cells) and LY-S (S cells)[27] with known telomere lengths of 80 and 10 kb, respectively (E. Samper and M.A.B., unpublished results). There was a linear correlation ($r^2 = 0.999$) between the fluorescence intensity of the R and S telomeres with a slope of 38.6. The calibration-corrected telomere fluorescence intensity was calculated as described[28]. We recorded the images using a COHU CCD camera on a fluorescence microscope (DMRb, Leica). A mercury vapor lamp (CS 100 W-2; Philips) was used as source. We captured the images using the Leica Q-FISH software at 400-ms integration time in a linear acquisition mode to prevent oversaturation of fluorescence intensity. We used the TFL-Telo software[29] to quantify the fluorescence intensity of telomeres from at least 10 metaphases for each data point. For chromosomal aberrations, we analyzed approximately 50 metaphases for each data point as described[9,17,28]. All metaphases were captured on the same day, in parallel and blindly. All the images from the MEFs were captured within 3 d after the hybridization.

Telomerase assay. We used a modified version of the telomeric repeat amplification protocol to measure telomerase activity on S-100 extracts from all the MEFs that we studied as described[7]. A control for PCR efficiency, IC, was included in each reaction (TRAPeze kit, Oncor).

Immunofluorescence. For immunostaining with antibodies against Terf1, we seeded 2×10^4 cells in multiwell immunofluorescence slides (Lab-Tek). After 24 h in culture, we washed the cells twice with PBS and fixed them in 4% paraformaldehyde/PBS for 20 min. Cells were then washed twice with PBS and treated with 0.1% Triton X-100 in PBS at 25 °C for 15 min followed by two washes with PBS. After blocking with 2% BSA in PBS at 4 °C overnight, we incubated the cells with rabbit polyclonal antibody against mouse Terf1 (#644; gift from T. de Lange) diluted 1:200 in PBS containing 2% BSA for 1 h at 25 °C. After two washes with PBS/0.05% Triton X-100, we incubated the cells for 1 h at 25 °C with secondary goat antibody against rabbit IgG conjugated with Cy3 and diluted 1:400 in PBS/2% BSA. After two PBS washes, slides were counterstained with 4′,6-diamidino-2 phenylindole (DAPI; 0.2 μg ml^{-1}) in Vectashield (Vector Laboratories). We recorded the images using a COHU CCD camera on a fluorescence microscope (DMRb, Leica). A mercury vapor lamp (CS 100 W-2; Philips) was used as light source. We captured the images using the Leica Q-FISH software at 400-ms integration time in a linear acquisition mode to prevent

Table 3 • Frequency of chromosomal aberrations per metaphase in increasing passages of TKO-A MEFs

TKO-A passage number	Number of metaphases	Telomere fusions (dicentrics)	Telomere fusions (robertsonian-like)	% metaphases with normal telomeres
p0	47	0	0	87
p2	48	0	0	71
p4	46	0	0	48
p6	51	0	0	16
p9	49	0.02	0	0
p11	49	0	0	0

oversaturation of fluorescence intensity. TFL-Telo software (gift from P. Lansdorp) was used to quantify the fluorescence intensity of Terf1 spots from at least 40 interphase nuclei.

Acknowledgments

We thank T. Jacks and J. Sage for the donation of numerous vials of TKO and DKO MEFs, B. Deberman and S. Weintraub for the gift of $Rb1^{-/-}$ and $Rb1^{+/+}$ MEFs and M. Serrano for critical reading of the manuscript and helpful discussions. M.G.-C. is a predoctoral fellow from the Spanish Ministry of Science and Technology. S.G. is supported by the US National Institutes of Health. Research at the laboratory of M.A.B. is funded by the Spanish Ministry of Science and Technology, the Regional Government of Madrid, the European Union and the Department of Immunology and Oncology (Spanish Research Council/Pharmacia Corporation).

Competing interests statement

The authors declare that they have no competing financial interests.

Received 19 June; accepted 20 August 2002.

1. Blackburn, E.H. Switching and signaling at the telomere. *Cell* **106**, 661–673 (2001).
2. Chan, S.W.-L. & Blackburn, E.H. New ways not to make ends meet: telomerase, DNA damage proteins and heterochromatin. *Oncogene* **21**, 553–563 (2002).
3. de Lange, T. Protection of mammalian telomeres. *Oncogene* **21**, 532–540 (2002).
4. Goytisolo, F.A. & Blasco, M.A. Many ways to telomere dysfunction: *in vivo* studies using mouse models. *Oncogene* **21**, 584–591 (2002).
5. Harley, C.B., Futcher, A.B. & Greider, C.W. Telomeres shorten during ageing of human fibroblasts. *Nature* **31**, 458–460 (1990).
6. Collins, K. & Mitchell, J.R. Telomerase in the human organism. *Oncogene* **21**, 564–579 (2002).
7. Blasco, M.A. *et al.* Telomere shortening and tumor formation by mouse cells lacking telomerase RNA. *Cell* **91**, 25–34 (1997).
8. Lee, H.-W. *et al.* Essential role of mouse telomerase in highly proliferative organs. *Nature* **392**, 569–574 (1998).
9. Samper, E., Flores, J.M. & Blasco, M.A. Restoration of telomerase activity rescues chromosomal instability and premature aging in *Terc*$^{-/-}$ mice with short telomeres. *EMBO Reports* **2**, 800–807 (2001).
10. Hemann, M.T., Strong, M.A., Hao, L.Y. & Greider, C.W. The shortest telomere, not average telomere length, is critical for cell viability and chromosome stability. *Cell* **107**, 67–77 (2001).
11. Bodnar, A.G. *et al.* Extension of life-span by introduction of telomerase into normal human cells. *Science* **279**, 349–352 (1998).
12. Kiyono, T. *et al.* Both Rb/p16^{INK4a} inactivation and telomerase activity are required to immortalize human epithelial cells. *Nature* **396**, 84–88 (1998).
13. Farwell, D.G. *et al.* Genetic and epigenetic changes in human epithelial cells immortalized by telomerase. *Am. J. Pathol.* **156**, 1537–1547 (2000).
14. Stoppler, H., Hartmann, D.P., Sherman, L. & Schlegel, R. The human papillomavirus type 16 E6 and E7 oncoproteins dissociate cellular telomerase activity from the maintenance of telomere length. *J. Biol. Chem.* **272**, 13332–13337 (1997).
15. Sage, J. *et al.* Targeted disruption of the three Rb-related genes leads to loss of G_1 control and immortalization. *Genes Dev.* **14**, 3037–3050 (2000).
16. van Steensel, B., Smogorzewska, A. & de Lange, T. TRF2 protects human telomeres from end-to-end fusions. *Cell* **92**, 401–413 (1998).
17. Samper, E., Goytisolo, F., Slijepcevic, P., van Buul, P. & Blasco, M.A. Mammalian Ku86 prevents telomeric fusions independently of the length of TTAGGG repeats and the G-strand overhang. *EMBO Reports* **1**, 244–252 (2000).
18. Goytisolo, F., Samper, E., Edmonson, S., Taccioli, G.E. & Blasco, M.A. Absence of DNA-PKcs in mice results in anaphase bridges and in increased telomeric fusions with normal telomere length and G-strand overhang. *Mol. Cell. Biol.* **21**, 3642–3651 (2001).
19. Hande, P.M., Samper, E., Lansdorp, P. & Blasco, M.A. Telomere length dynamics in cultured cells from normal and telomerase-null mice. *J. Cell Biol.* **144**, 589–601 (1999).
20. Chong, L. *et al.* A human telomeric protein. *Science* **270**, 1663–1667 (1995).
21. Smogorzewska, A. *et al.* Control of human telomere length by TRF1 and TRF2. *Mol. Cell. Biol.* **20**, 1659–1668 (2000).
22. van Steensel, B. & de Lange, T. Control of telomere length by the human telomeric protein TRF1. *Nature* **385**, 740–743 (1997).
23. Espejel, S. *et al.* Mammalian Ku86 mediates chromosomal fusions and apoptosis caused by critically short telomeres. *EMBO J.* **21**, 2207–2219 (2002).
24. Henson, J.D., Neumann, A.A., Yeager, T.R. & Reddel, R.R. Alternative lengthening of telomeres in mammalian cells. *Oncogene* **21**, 598–610 (2002).
25. Perrem, K., Colgin, L.M., Neumann, A.A., Yeager, T.R. & Reddel, R.R. Co-existence of alternative lengthening of telomeres and telomerase in hTERT-transfected GM847 cells. *Mol. Cell. Biol.* **21**, 3862–3875 (2001).
26. Murga, M. *et al.* Mutation of the E2F2 in mice causes enhanced T lymphocyte proliferation, leading to the development of autoimmunity. *Immunity* **15**, 959–970 (2001).
27. McIlrath, J.S. *et al.* Telomere length abnormalities in mammalian radiosensitive cells. *Cancer Res.* **61**, 912–915 (2001).
28. Herrera, E. *et al.* Disease states associated with telomerase deficiency appear earlier in mice with short telomeres. *EMBO J.* **18**, 2950–2960 (1999).
29. Zijlmans, J.M. *et al.* Telomeres in the mouse have large inter-chromosomal variations in the number of T2AG3 repeats. *Proc. Natl Acad. Sci. USA* **94**, 7423–7428 (1997).